



Influence of the Front-Rear Torque Distribution on the Handling Characteristics and Stability Boundaries of an AWD-Vehicle

Manuel Eberhart¹(✉), Martin Arndt², Johannes Edelmann¹,
and Manfred Plöchl¹

¹ TU Wien, Institute of Mechanics and Mechatronics, Vienna, Austria

manuel.eberhart@tuwien.ac.at

² CARIAD SE, Vehicle Motion Energy, Wolfsburg, Germany

martin.arndt@cariad.technology

<https://www.mec.tuwien.ac.at/vsd>, <https://www.cariad.technology>

Abstract. The influence of the drive torque distribution of an AWD vehicle with individual motors at the front and rear axles on the handling and stability properties is investigated. By applying bifurcation analysis methods, different types of loss of stability at combined longitudinal and lateral acceleration are identified. The impact of the drive torque distribution on the stability boundaries in the GG diagram is examined, and the related stable acceleration envelope is compared to the envelope derived from applying optimisation methods. Representative corresponding handling characteristics are compared and discussed.

Keywords: Handling Characteristics · Stability · Bifurcation · Drive Torque Distribution · Optimisation · AWD Vehicle

1 Introduction

Drive train architectures of electric vehicles, often equipped with more than one electric motor, allow both to ‘stabilise’ and to make the vehicle’s motion ‘more responsive’ but also require a profound understanding of its influence on stability and handling to ensure safe operation. Depending on the longitudinal acceleration and drive train configuration, the handling behaviour and respective passive stability properties of the vehicle can significantly change [1, 5, 6]. To study these characteristic properties, a quasi-steady-state description is derived, where the state of a vehicle accelerated in longitudinal direction is transformed to a mechanically equivalent steady-state [1, 6].

Bifurcation analysis is frequently used to find stability boundaries [10]. In [3], Della Rossa et al. analyse the stability properties of a vehicle with different tyre configurations and demonstrate that various types of loss of stability may appear. Horiuchi et al. use a quasi-steady-state description to model transient states to investigate the loss of stability for a longitudinally accelerated vehicle

with fixed drive torque distribution in [5]. Lenzo et al. analyse the handling characteristics for different drive concepts and present the relation between yaw torque and understeer coefficient [7].

This paper investigates the impact of the drive torque distribution of an AWD vehicle with individual motors at the front and rear axles on the transient handling and stability properties. The vehicle state is transformed to a mechanically equivalent quasi-steady-state to apply linear stability theory and to utilise bifurcation and continuation algorithms. For various drive torque distributions, different types of bifurcations are found and discussed. The stable acceleration envelope is compared to the solution found by optimisation, and differences are discussed.

The paper is structured as follows: In the next Section, the vehicle and tyre models are addressed. In Sect. 3, the applied methods are briefly described. In the following Sect. 4, the impact of the longitudinal acceleration on the handling characteristics is shown. The stability boundary found with the bifurcation method is presented in the GG diagram and compared to the optimised acceleration envelope in Sect. 5.

2 Vehicle Model

A nonlinear four-wheel vehicle model with 10 degrees of freedom, as introduced and described in [4] and illustrated in Fig. 1, is considered in this study. The rigid vehicle body is modelled with 6 degrees of freedom, (longitudinal velocity v_{xB} , lateral velocity v_{yB} , vertical velocity v_{zB} , roll angle φ_B , pitch angle θ_B and yaw rate $\dot{\psi}_B$), and one rotational degree of freedom is considered for each wheel, ω_i ($i = 1, 2, 3, 4$). Input quantities are the drive torques at the individual wheels, $T_1 = T_2$ and $T_3 = T_4$, and the steering angle δ , where $\delta_1(\delta)$ and $\delta_2(\delta)$. The Magic Formula [9] is used to model the combined tyre force characteristics. In the subsequent figures, the vehicle states are represented in the x - y - z -coordinate frame depicted in red colour in Fig. 1.

For vehicle parameters, governing equations and tyre force characteristics, please refer to [4].

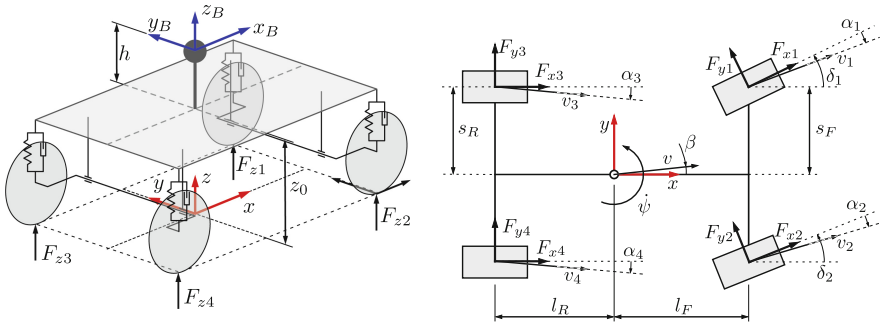


Fig. 1. Schematic illustration of the vehicle model

3 Methods

To apply continuation methods for the nonlinear stability analysis, the combined accelerated manoeuvre ($a_n \neq 0$ and $a_t \neq 0$) is transformed to a quasi-steady-state, mechanically equivalent state, which approximates the combined acceleration manoeuvre well [2, 5]. In this paper, similar to [5], an equivalent force in the direction of the velocity vector is applied at the centre of gravity of the vehicle. This system adaption considers both the load transfer and the mutual influence of the longitudinal and lateral tyre forces. Yaw acceleration $\dot{\psi}$, derivative of the vehicle sideslip angle $\dot{\beta}$, and the derivatives of the other states are set to zero to fulfil the steady-state condition.

Once equivalent equilibrium solutions are found, linear methods are applied to analyse stability properties. For that purpose, the equations of motion are linearised with respect to the equilibrium solutions, $\Delta \dot{\mathbf{x}} = \mathbf{A} \Delta \mathbf{x} + \mathbf{B} \Delta \mathbf{u}$. Lyapunov's first method implies that an equilibrium solution is stable if all eigenvalues λ_i from $(\mathbf{A} - \lambda_i \mathbf{I}) \mathbf{p}_i = \mathbf{0}$, with the right eigenvector \mathbf{p}_i , have negative real parts [10].

With the help of a path continuation algorithm [10], solution paths are found by varying parameters and inputs. A more detailed description of the used method is given in [4]. Moreover, optimisation techniques are applied to find the maximum possible acceleration envelope [8]. The result is compared to the stable acceleration envelope found with bifurcation analysis.

4 Handling Characteristics at Longitudinal Acceleration

The handling diagram for the considered vehicle with drive torque distribution $\gamma = 1$, i.e. rear-wheel-drive (RWD), and zero tangential acceleration shows understeer handling characteristics and limit understeer behaviour, see Fig. 2 (blue line). The respective vehicle configuration with $\gamma = 0$, i.e. front-wheel-drive (FWD), shows qualitatively the same characteristics and is not depicted.

Increasing the vehicle tangential acceleration, e.g. to $a_t = 4 \text{ m/s}^2$, results in a qualitative change to limit oversteer behaviour of the vehicle with $\gamma = 1$ (Fig. 2, orange line). In contrast, no qualitative change may be observed for $\gamma = 0$ (not depicted) and an all-wheel-drive (AWD) configuration with a certain portion of drive torque at the front axle (e.g. $\gamma = 0.7$, green line).

Evaluating the eigenvalues for $\gamma = 1$ at $a_t = 4 \text{ m/s}^2$ indicates a Hopf-type loss of stability (o in Fig. 2), characterised by a conjugate complex pair of eigenvalues with zero real part. For decreased parameter γ the Hopf point moves to higher normal accelerations a_n (black line) while the imaginary part of the Hopf eigenvalue λ_I decreases and finally results in two zero eigenvalues, Fig. 2 black x, called Takens–Bogdanov bifurcation. Further decrease of the drive torque distribution γ leads to limit understeer behaviour. The torque distribution at the Takens–Bogdanov point, $\gamma_{\text{TB}} \approx 0.86$ for a tangential acceleration of $a_t = 4 \text{ m/s}^2$, characterises the change from limit understeer to limit oversteer behaviour and vice versa. The Takens–Bogdanov solution for various γ and a_t is depicted in Fig. 2 (red line).

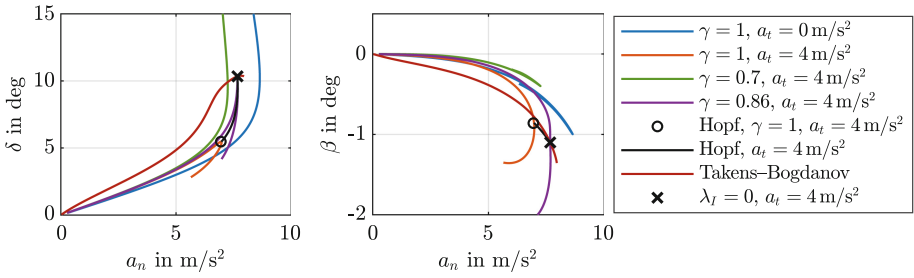


Fig. 2. Steering angle δ and vehicle sideslip angle β for different drive torque distributions γ at tangential acceleration a_t . Quasi-steady-state solutions for vehicle velocity $v = 20 \text{ m/s}^2$.

5 Takens–Bogdanov Point as Design Criteria

The corresponding a_x – a_y diagram (GG diagram) depicted in the left graph of Fig. 3 includes two coloured lines: the maximum lateral acceleration for the considered vehicle with $\gamma = 1$ (blue line) that shows limit understeer behaviour up to a longitudinal acceleration of $a_x = 2.6 \text{ m/s}^2$, followed by the Takens–Bogdanov solution for higher longitudinal accelerations (red line). In the right graph of Fig. 3 (red line), the respective torque distribution γ for the Takens–Bogdanov solution is plotted over the longitudinal acceleration a_x .

In addition, the numerically optimised GG diagram that represents the maximum acceleration envelope for the considered vehicle and the resulting optimisation parameter γ are plotted in Fig. 3 (black lines).

In the left graph, it can be seen that the solutions from bifurcation analysis and optimisation are almost equal. Nevertheless, at small longitudinal accelerations $a_x < 2.5 \text{ m/s}^2$ the maximum lateral accelerations a_y from the optimised drive torque distribution γ are slightly superior. Inspecting the respective drive torque distributions γ , right graph in Fig. 3, shows that an AWD configuration is beneficial in this regime.

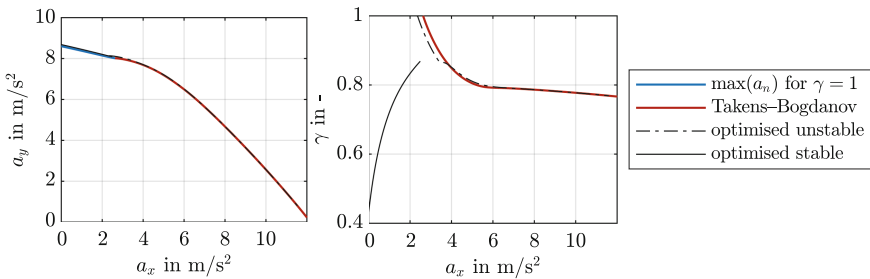


Fig. 3. Comparison of Takens–Bogdanov solution and optimised solution: Acceleration envelope a_x – a_y and drive torque distribution γ .

Considering the graph of the optimal drive torque distribution γ , at $a_x \approx 2.5$ m/s² a discontinuity can be noticed. Evaluating the stability properties of the steady-state solutions derived with the optimisation technique reveals a qualitative change from stable conditions (black solid line) to unstable conditions (black dashed-dotted line) at $a_x > 2.5$ m/s², whereas the Takens–Bogdanov solution characterises the stability boundary in the a_x – a_y -envelope. This can also be seen in Fig. 4 where handling curves for three constant tangential accelerations $a_t = 1, 3, 5$ m/s² are plotted for the respective optimal and Takens–Bogdanov quasi-steady-state solutions, and corresponding constant drive torque distributions γ_{opt} and γ_{TB} , respectively.

The handling curves for $a_t = 1$ m/s² show that the maximum normal acceleration a_n of the optimised solution is superior compared to the $\gamma = 1$ configuration. For $a_t = 3$ m/s² the optimal solution is found for $\gamma_{\text{opt}} < \gamma_{\text{TB}}$ after loss of stability (Fold bifurcation). The Fold bifurcation occurs after limit understeer behaviour and can be attributed to the saturation of the longitudinal tyre forces at the inner rear wheel ($i = 3$). The behaviour then changes to an unstable oversteer behaviour where the optimal solution is found.

At tangential acceleration $a_t = 5$ m/s² the torque distribution of the optimised solution is a little larger than the torque distribution of the Takens–Bogdanov point ($\gamma_{\text{opt}} > \gamma_{\text{TB}}$) and a slightly higher normal acceleration a_n is achieved. The optimised quasi-steady-state solution is again unstable following a Hopf bifurcation.

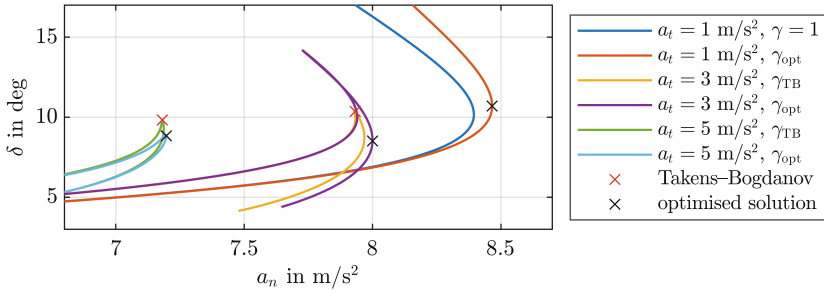


Fig. 4. Detail of handling diagram for different constant tangential accelerations a_t and drive torque distributions γ .

6 Conclusions

The transition between limit understeer and limit oversteer behaviour due to the change of the drive torque distribution at longitudinal acceleration in quasi-steady-state condition was investigated. It was shown that the Takens–Bogdanov solution characterises both the change from limit oversteer to limit understeer

behaviour and the change of the type of loss of stability from Hopf to Fold bifurcation.

A Takens–Bogdanov solution was identified by Della Rossa et al. in [3] by studying a pure lateral vehicle model with the same maximum friction potential of the tyres at the front and rear axles. In this study, it was shown that a similar behaviour may result from the mutual influence of longitudinal and lateral tyre forces at a vehicle accelerated in longitudinal direction.

The Takens–Bogdanov solution seems to be a reasonable design criterion for the drive torque distribution of an AWD vehicle since, for a given longitudinal acceleration (or an equivalent drive torque demand), almost the maximum normal acceleration may be achieved without ‘early’ limit understeer or oversteer behaviour. This may improve the vehicle’s safety and manoeuvrability during combined manoeuvres. In addition, the Takens–Bogdanov solution represents the acceleration envelope near the optimal (maximal) envelope. In contrast to the latter, which includes unstable solutions, the Takens–Bogdanov solution may be of more practical relevance, since the solutions are stable. However, potential practical implications have to be investigated thoroughly. The impact of relevant system parameters like tyre–road friction potential and different vehicle parameters have to be considered, and their influence on the shown method should be analysed.

Further investigations on the drive torque distribution to generate yaw torque to modify the handling behaviour and stability boundaries appear to be reasonable. This will be studied in more detail in a forthcoming paper.

References

1. Abe, M.: A theoretical analysis on vehicle cornering behaviors in acceleration and in braking. *Veh. Syst. Dyn.* **15**(1), 1–14 (1986). <https://doi.org/10.1080/00423118608969122>
2. De Novellis, L., Sorniotti, A., Gruber, P.: Optimal wheel torque distribution for a four-wheel-drive fully electric vehicle. *SAE Int. J. Passeng. Cars Mech. Syst.* **6**(1), 128–136 (2013). <https://doi.org/10.4271/2013-01-0673>
3. Della Rossa, F., Mastinu, G., Piccardi, C.: Bifurcation analysis of an automobile model negotiating a curve. *Veh. Syst. Dyn.* **50**(10), 1539–1562 (2012). <https://doi.org/10.1080/00423114.2012.679621>
4. Eberhart, M., Plöchl, M., Edelmann, J.: Stability boundaries and bifurcation analysis of an AWD vehicle with variable drive torque distribution. To be submitted to *Nonlinear Dynamics* (2024)
5. Horiuchi, S., Okada, K., Nohtomi, S.: Analysis of accelerating and braking stability using constrained bifurcation and continuation methods. *Veh. Syst. Dyn.* **46**(1), 585–597 (2008). <https://doi.org/10.1080/00423110802007779>
6. Klomp, M., Thomson, R.: Influence of front/rear drive force distribution on the lateral grip and understeer of all-wheel drive vehicles. *Int. J. Veh. Des.* **56**(1–4), 34–48 (2011). <https://doi.org/10.1504/IJVD.2011.043272>
7. Lenzo, B., Bucchi, F., Sorniotti, A., Frendo, F.: On the handling performance of a vehicle with different front-to-rear wheel torque distributions. *Veh. Syst. Dyn.* **57**(11), 1685–1704 (2019). <https://doi.org/10.1080/00423114.2018.1546013>

8. Massaro, M., Limebeer, D.J.N.: Minimum-lap-time optimisation and simulation. *Veh. Syst. Dyn.* **59**(7), 1069–1113 (2021). <https://doi.org/10.1080/00423114.2021.1910718>
9. Pacejka, H.: *Tire and Vehicle Dynamics*. Elsevier, Amsterdam (2005)
10. Seydel, R.: Practical bifurcation and stability analysis. In: *Interdisciplinary Applied Mathematics*, vol. 5. Springer, Cham (2009). <https://doi.org/10.1007/978-1-4419-1740-9>

Open Access This chapter is licensed under the terms of the Creative Commons Attribution 4.0 International License (<http://creativecommons.org/licenses/by/4.0/>), which permits use, sharing, adaptation, distribution and reproduction in any medium or format, as long as you give appropriate credit to the original author(s) and the source, provide a link to the Creative Commons license and indicate if changes were made.

The images or other third party material in this chapter are included in the chapter's Creative Commons license, unless indicated otherwise in a credit line to the material. If material is not included in the chapter's Creative Commons license and your intended use is not permitted by statutory regulation or exceeds the permitted use, you will need to obtain permission directly from the copyright holder.

